

AD-A137 095

EFFECTIVE EARTH RADIUS FOR REFRACTION OF RADIO WAVES AT 1/1  
ALTITUDES ABOVE 1 KM(U) MITRE CORP BEDFORD MA  
G A ROBERTSHAW DEC 83 MTR-8915 ESD-TR-83-219

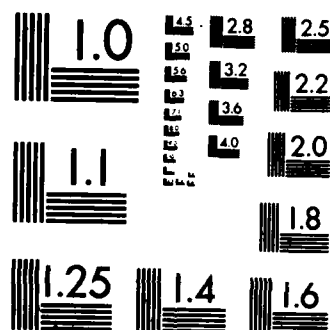
UNCLASSIFIED

F19628-82-C-0001

F/G 20/14

NL

END



MICROCOPY RESOLUTION TEST CHART  
NATIONAL BUREAU OF STANDARDS-1963-A

12

AD A137095

**EFFECTIVE EARTH RADIUS FOR REFRACTION  
OF RADIO WAVES AT ALTITUDES ABOVE 1 KM**

By  
**G. A. ROBERTSHAW**

**DECEMBER 1983**

Prepared for  
**DEPUTY FOR TACTICAL SYSTEMS  
ELECTRONIC SYSTEMS DIVISION  
AIR FORCE SYSTEMS COMMAND  
UNITED STATES AIR FORCE  
Hanscom Air Force Base, Massachusetts**



**DTIC**  
**ELECTE**  
**JAN 23 1984**  
**E**

**DTIC FILE COPY**

Approved for public release;  
distribution unlimited.

Project No. 6460  
Prepared by  
**THE MITRE CORPORATION**  
Bedford, Massachusetts  
Contract No. F19628-82-C-0001

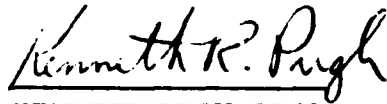
84 01 19 030

When U.S. Government drawings, specifications, or other data are used for any purpose other than a definitely related government procurement operation, the government thereby incurs no responsibility nor any obligation whatsoever; and the fact that the government may have formulated, furnished, or in any way supplied the said drawings, specifications, or other data is not to be regarded by implication or otherwise, as in any manner licensing the holder or any other person or corporation, or conveying any rights or permission to manufacture, use, or sell any patented invention that may in any way be related thereto.

Do not return this copy. Retain or destroy.

### REVIEW AND APPROVAL

This technical report has been reviewed and is approved for publication.



KENNETH PUGH, GS-12  
Project Engineer

FOR THE COMMANDER



DONALD W. DILL, Colonel, USAF  
Deputy for Tactical Systems

UNCLASSIFIED

AD-A137095

SECURITY CLASSIFICATION OF THIS PAGE

## REPORT DOCUMENTATION PAGE

1a. REPORT SECURITY CLASSIFICATION Unclassified			1b. RESTRICTIVE MARKINGS		
2a. SECURITY CLASSIFICATION AUTHORITY			3. DISTRIBUTION/AVAILABILITY OF REPORT  Approved for public release; distribution unlimited.		
2b. DECLASSIFICATION/DOWNGRADING SCHEDULE					
4. PERFORMING ORGANIZATION REPORT NUMBER(S) MTR-8915 ESD-TR-83-219			5. MONITORING ORGANIZATION REPORT NUMBER(S)		
6a. NAME OF PERFORMING ORGANIZATION  The MITRE Corporation		6b. OFFICE SYMBOL (If applicable)		7a. NAME OF MONITORING ORGANIZATION	
6c. ADDRESS (City, State and ZIP Code)  Burlington Road Bedford, MA 01730			7b. ADDRESS (City, State and ZIP Code)		
8a. NAME OF FUNDING/SPONSORING ORGANIZATION  Deputy for Tactical Systems		8b. OFFICE SYMBOL (If applicable)  TCG		9. PROCUREMENT INSTRUMENT IDENTIFICATION NUMBER  F19628-82-C-0001	
8c. ADDRESS (City, State and ZIP Code)  Electronic Systems Division, AFSC Hanscom AFB, MA 01731			10. SOURCE OF FUNDING NOS.		
			PROGRAM ELEMENT NO.	PROJECT NO.  6460	TASK NO.
			WORK UNIT NO.		
11. TITLE (Include Security Classification) EFFECTIVE EARTH RADIUS FOR REFRACTION OF RADIO WAVES AT ALTITUDES ABOVE 1 KM					
12. PERSONAL AUTHOR(S) G. A. Robertshaw					
13a. TYPE OF REPORT  Final Report		13b. TIME COVERED FROM _____ TO _____		14. DATE OF REPORT (Yr., Mo., Day) 1983 December	
15. PAGE COUNT 40					
16. SUPPLEMENTARY NOTATION					
17. COSATI CODES			18. SUBJECT TERMS (Continue on reverse if necessary and identify by block number)		
FIELD	GROUP	SUB. GR.	EFFECTIVE EARTH RADIUS RAY TRACE		
			MICROWAVE PROPAGATION REFRACTIVITY		
19. ABSTRACT (Continue on reverse if necessary and identify by block number)  Atmospheric refractivity gradients are responsible for the bending of radio and microwave propagation paths such that the electromagnetic line-of-sight deviates from the geometrical line-of-sight. Such refraction effects must be accounted for when the performance of airborne surveillance radar systems is modelled. For propagation paths within 1 kilometer of the earth's surface, the effective earth radius model, which accounts for bending of rays by rescaling the earth's radius, is normally valid and commonly used. In the present work, a ray trace method for determination of propagation paths in a semi-empirical stratified atmosphere is described. Results obtained from the ray trace model are employed to show that the effective earth radius method can be used for approximate determinations of grazing angle, ground range, and slant range for higher altitude paths. Effective earth radius scale factors are given as a function of transmitter altitude for selected values of surface refractivity. However, it must be emphasized that very accurate propagation prediction still requires detailed ray trace calculations in the context of accurate atmospheric models.					
20. DISTRIBUTION/AVAILABILITY OF ABSTRACT  UNCLASSIFIED/UNLIMITED <input type="checkbox"/> SAME AS RPT <input checked="" type="checkbox"/> DTIC USERS <input type="checkbox"/>			21. ABSTRACT SECURITY CLASSIFICATION  Unclassified		
22a. NAME OF RESPONSIBLE INDIVIDUAL  Susan R. Gilbert			22b. TELEPHONE NUMBER (Include Area Code) (617) 271-8088		22c. OFFICE SYMBOL

## TABLE OF CONTENTS

<u>Section</u>	<u>Page</u>
LIST OF ILLUSTRATIONS	2
LIST OF TABLES	3
ACKNOWLEDGMENTS	4
1 INTRODUCTION	5
2 DESCRIPTION OF RAY TRACE AND EFFECTIVE EARTH RADIUS METHODS	7
3 RESULTS: A COMPARISON OF RAY TRACE AND EFFECTIVE EARTH RADIUS PREDICTIONS	15
4 CONCLUSIONS	31
LIST OF REFERENCES	32
APPENDIX SEMI-EMPIRICAL ATMOSPHERIC REFRACTIVITY MODEL	33

Accession For	
NTIS GRA&I	<input checked="" type="checkbox"/>
DTIC TAB	<input type="checkbox"/>
Unannounced	<input type="checkbox"/>
Justification	
By	
Distribution/	
Availability Codes	
Dist	Avail and/or Special
<div style="font-size: 2em; font-weight: bold; position: absolute; left: 5px; bottom: 5px;">A-1</div>	



## LIST OF ILLUSTRATIONS

<u>Figure</u>	<u>Page</u>
1     Atmospheric Ray Trace Exponential Shell Model	8
2     Effective Earth Radius Geometry	12
3     Range Versus Initial Depression Angle for Source at 15 kft., Terrain Elevation of 1 kft. and $N_s = 300$	20
4     Range Versus Initial Depression Angle for Source at 45 kft., Terrain Elevation of 1 kft. and $N_s = 300$	21
5     Range Versus Initial Depression Angle for Source at 60 kft., Terrain Elevation of 1 kft. and $N_s = 300$	22
6     Grazing Angle Versus Depression Angle for Source at 45 kft., Terrain Elevation of 1 kft. and $N_s = 300$	23
7     Effective Earth Radius Factor Versus Source Altitude for $N_s = 200, 300$ and 400	26
8     Ray Trace Versus Effective Earth Radius Model Ground Range for Higher Altitude Paths	27
9     Ray Trace Versus Effective Earth Radius Model Ground Range for Lower Altitude Paths	28
A-1   Refractivity Profiles: 1-30 kft. MSL	36
A-2   Refractivity Profile: 30-90 kft. MSL	37
A-3   Refractivity Gradient Versus Altitude	38

## LIST OF TABLES

<u>Table</u>		<u>Page</u>
1	Model Comparison for Source at 15 kft., Surface at 1 kft. and $N_s = 300$	16
2	Model Comparison for Source at 45 kft., Surface at 1 kft. and $N_s = 300$	17
3	Model Comparison for Source at 60 kft., Surface at 1 kft. and $N_s = 300$	18
4	Effective Earth Radius Factor Versus Source Altitude and Surface Refractivity for 1 kft. Terrain Elevation	24
5	Effective Earth Radius Factor Versus Source Altitude and Surface Refractivity for 2 kft. Terrain Elevation	30



## ACKNOWLEDGMENTS

The author wishes to thank M. M. Weiner for useful suggestions generated in the course of this work, and E. W. Beasley and L. P. Shepherd for their thorough review of the manuscript.

This document has been prepared by The MITRE Corporation under Project 6460, Contract F19628-82-C-0001. The contract is sponsored by the Electronic Systems Division, Air Force Systems Command, Hanscom Air Force Base, Massachusetts.

## SECTION 1

### INTRODUCTION

Under normal circumstances, the density of the earth's atmosphere decreases monotonically with increasing altitude.<sup>1</sup> This vertical density gradient, with the addition of a highly variable contribution due to the water vapor component, is responsible for a gradient in the index of refraction at radio and microwave frequencies. Typically, electromagnetic waves in the atmosphere will bend downwards, i.e., towards the denser medium. For a generalized atmosphere whose refractivity is a function of three dimensions, elaborate mathematical procedures are necessary to predict the propagation path of radio waves with reasonable confidence. If the refractivity gradient is constant and vertical everywhere, which corresponds to a stratified atmosphere in which the refractivity decreases linearly with altitude, the elegant and widely used effective earth radius method<sup>2</sup> (EERM) may be employed to obtain geometrical quantities which characterize the propagation path, e.g., earth grazing angle. Since the EERM is predicated upon average atmospheric conditions, it remains unsuitable for highly accurate prediction of propagation paths if detailed atmospheric data can be used in a ray trace analysis.

The EERM allows the propagation of radio waves to be represented by straight lines if an appropriate factor is used to scale the earth's radius as measured to the terrain above which propagation occurs. When the correct scale factor is used, slant range, grazing angle and ground range are identical to the true curved path values, but can, however, be reckoned easily using straight lines. Although the EERM is simple to use, its accuracy hinges upon the scale factor used, and it is limited to stratified atmospheres which do not exhibit excessive anomalies, e.g., thermal inversions, inhomogeneities, etc. Despite these reservations, radar performance analysts routinely adopt a scale factor which can vary from  $\sim 1.1$  to  $\sim 1.8$ , depending upon season and geographic location.\* The often quoted factor of  $4/3$  is sometimes used as a very general "rule of thumb" by those who lack detailed data or wish to consider only the general propagation environment.

\*This range of scale factors should not be confused with scale factor altitude dependence at a given location.

For approximate work, it would be desirable to maintain the simplicity of the EERM, while extending the range of the method to higher altitudes for which the refractivity profile is exponential rather than linear. The purpose of the present work is to show that suitable scale factors can be determined and employed to yield reasonable approximations for path parameters at higher altitudes. In general, the scale factor is strongly dependent upon the source (transmitter) altitude and surface refractivity. The above findings are based on numerical ray trace computations performed in the context of a semi-empirical refractivity profile, as described in detail in the next section.

It should be emphasized that the EERM is no substitute for the detailed atmospheric modeling and ray trace techniques required for very accurate propagation path prediction.

In section 3 results are presented which include scale factor versus source altitude curves and tables. Conclusions appear in section 4, while a description of the refractivity model is provided in the appendix.

## SECTION 2

### DESCRIPTION OF RAY TRACE AND EFFECTIVE EARTH RADIUS METHODS

Although a large body of literature exists on the subject of radio and microwave propagation in the atmosphere, a comprehensive review of this material is unnecessary to achieve the limited goals of the present work. Indeed, the ray trace computations outlined below require only elementary geometry, Snell's law, and a realistic atmospheric refractivity profile. The central purpose of this study is to investigate effective earth radius approximations for higher altitude paths and determine suitable scale factors. Other topics such as attenuation, electrical path length, and divergence are not addressed.

Consider a source of radio or microwaves (e.g., radar) at an altitude  $h_7$  above mean sea level (MSL) in a stratified atmosphere which lies above smooth spherical terrain with elevation  $h_s$  (MSL), as depicted in figure 1. Irregular terrain is also permissible provided that the terrain roughness is small relative to the lower concentric shell thickness,  $\Delta h$ . As illustrated in the figure (exaggerated for clarity), the spherically symmetric atmosphere is divided into a set of 7 shells such that the thickness ratio of adjacent shells is constant. The first shell thickness ( $\Delta h$ ), and number of shells,  $M$ , ( $M = 7$  in figure 1) are independent parameters selected by the atmospheric modeler. These parameters, together with the total thickness ( $h_7 - h_s$ ), determine the adjacent shell thickness ratio,  $C$ , through,

$$h_7 - h_s = \frac{\Delta h(C^7 - 1)}{C - 1} \quad (1)$$

which can be solved numerically. The geometrical progression in shell thickness provides more shells at the lower altitudes, for which the refractivity gradient is generally larger, to improve the accuracy of the ray trace algorithm. For clarity, only 7 shells are illustrated in figure 1. In actual calculations, as many as 100 are used. Within each shell or stratum the refractivity is taken to be constant with a value specified by the semi-empirical refractivity function, described in the appendix, evaluated at the average shell altitude. Therefore, in the model, rectilinear propagation occurs within shells, while at

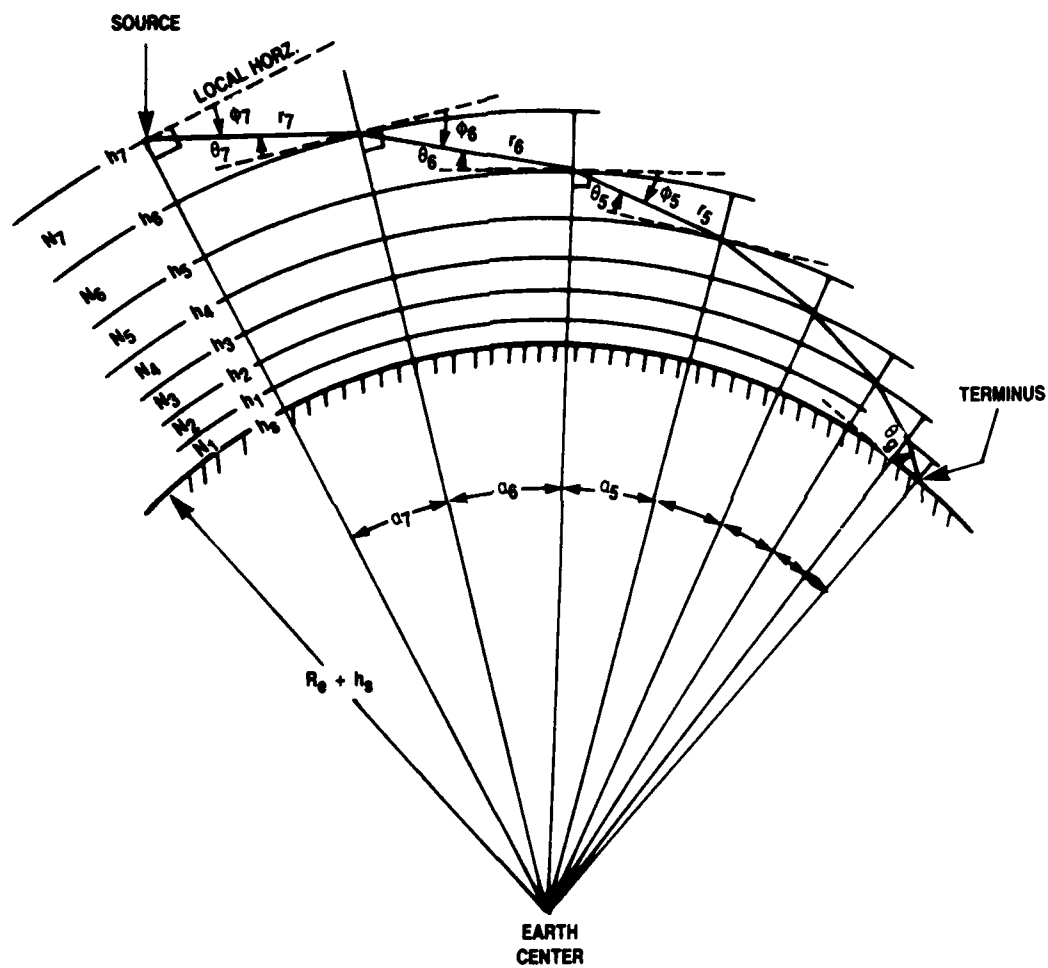


**Figure 1. Atmospheric Ray Trace Exponential Shell Model**

the boundaries Snell's law of refraction is invoked to account for ray bending. Ray tracing is performed as follows:

1. The initial ray elevation angle  $\phi_M$ , source height ( $h_M$ ), surface height ( $h_s$ ), number of shells ( $M$ ) and first shell thickness ( $\Delta h$ ) are specified.
2. The adjacent shell thickness ratio ( $C$ ) is obtained by numerical solution of equation 1. The thickness of the "mth" shell is then:

$$\Delta h_m = \Delta h C^{m-1} \quad (2)$$

3. The intersection of the ray with the first shell boundary, i.e., the boundary between shell  $M$  and  $M-1$ , is found by geometry. The quantities of interest are  $r_M$ ,  $\alpha_M$  and  $\theta_M$ .

The quantity  $r_M$  is the length of the segment of ray within shell  $M$  and is given by,

$$r_M = -(R_e + h_M) \sin \phi_M - \left[ \left[ (R_e + h_M) \sin \phi_M \right]^2 - \Delta h C^{M-1} \left[ 2(R_e + h_M) - \Delta h C^{M-1} \right] \right]^{\frac{1}{2}} \quad (3)$$

in which  $R_e$  is the nominal earth radius of 6,373 km. The angle  $\alpha_M$  is subtended at the earth's center by the endpoints of  $r_M$  and is given by,

$$\alpha_M = \sin^{-1} \left[ \frac{r_M \cos \phi_M}{R_e + h_M - \Delta h C^{M-1}} \right] \quad (4)$$

while the incidence angle at the lower shell boundary,  $\theta_M$ , is given by,

$$\theta_M = -\alpha_M - \phi_M \quad (5)$$

which is a positive quantity. This is true since only negative values of  $\phi_M$ , the initial elevation angle, are used,  $\alpha_M$  is always positive, and,

$$|\phi_M| > |\alpha_M| \quad (6)$$

from geometry.

4. At the first shell boundary the ray undergoes refraction in accordance with Snell's law (the interface is assumed to be locally flat). Thus, the elevation of the ray at the top of the lower shell is obtained from,

$$\phi_{M-1} = -\cos^{-1} \left[ \frac{n_M \cos \theta_M}{n_{M-1}} \right] \quad (7)$$

in which  $n_M$  is the refractive index of the upper shell and  $n_{M-1}$  is the refractive index of the lower shell. Note that  $\phi_{M-1}$ , like  $\phi_M$ , is a negative (elevation) angle. The refractive index within a shell is obtained from the refractivity profile  $N[h]$ , evaluated at the average shell altitude, for example;

$$n_M = 1 + N[h] \quad ; \quad h = h_M - \frac{\Delta h C^{M-1}}{2} \quad (8)$$

5. Steps (1) through (4) are repeated for shell  $M-1$  to determine  $r_{M-1}$ ,  $\alpha_{M-1}$  and  $\theta_{M-1}$ , and this procedure is carried out for the remaining shells, in sequence.

In the course of the computations outlined above, the intrashell segment lengths and their corresponding earth-center subtended angles are accumulated. For a large ( $\sim 100$ ) number of shells, the spatial slant range from source to surface is, to a very good approximation:

$$R_s \cong \sum_{m=1}^M r_m \quad (9)$$

The ground range from a point on the surface directly below the source to the terminus is given by,

$$R_g \cong (R_e + h_s) \sum_{m=1}^M \alpha_m \quad ; (\alpha_m \text{ in radians}) \quad (10)$$

The earth grazing angle,  $\theta_g$ , is simply the incidence angle at the lower boundary of the lowest shell, i.e., shell no. 1:

$$\theta_g = \theta_1 \quad (11)$$

Thus, for given values of source altitude ( $h_M$ ), terrain altitude ( $h_s$ ), and  $\phi_M$ , the ray trace propagation algorithm yields  $R_s$ ,  $R_g$  and  $\theta_g$ . On the other hand, it should be noted that for elevation angles larger than some critical value, which depends upon  $h_M$  and  $h_s$ , some ray segment fails to intersect a lower shell, and  $r_m$  as given by equation (2) is complex. In this case, the ray returns to upper shells and diverges from the earth's surface. Therefore, no earth grazing result exists for elevation angles above a critical value, which corresponds to the radio horizon, in the context of the shell model.

The EERM is a shortcut but rigorous means of taking into account atmospheric refraction at low altitudes, where the atmospheric refractivity profile is (ideally) linear. Under these circumstances, electromagnetic waves can be regarded as propagating along straight lines if the earth radius is properly scaled, and ground range, slant range and grazing angle have correct values.

Figure 2 illustrates, in an exaggerated manner, the EERM geometry. The scale factor,  $K$ , is applied to the earth's radius as measured to the surface over which propagation occurs. The calculation of  $R_s$ ,  $R_g$  and  $\theta_g$  is then analogous to that performed within a single shell for the ray trace model (equations (3), (4), and (5)):

$$R_s = - \left[ K(h_s + R_e) + h - h_s \right] \sin \phi - \left[ \left[ \left[ K(h_s + R_e) + h - h_s \right] \sin \phi \right]^2 - (h - h_s) \left[ 2 \left[ K(h_s + R_e) + h - h_s \right] - (h - h_s) \right] \right]^{\frac{1}{2}} \quad (12)$$



LA-46,881

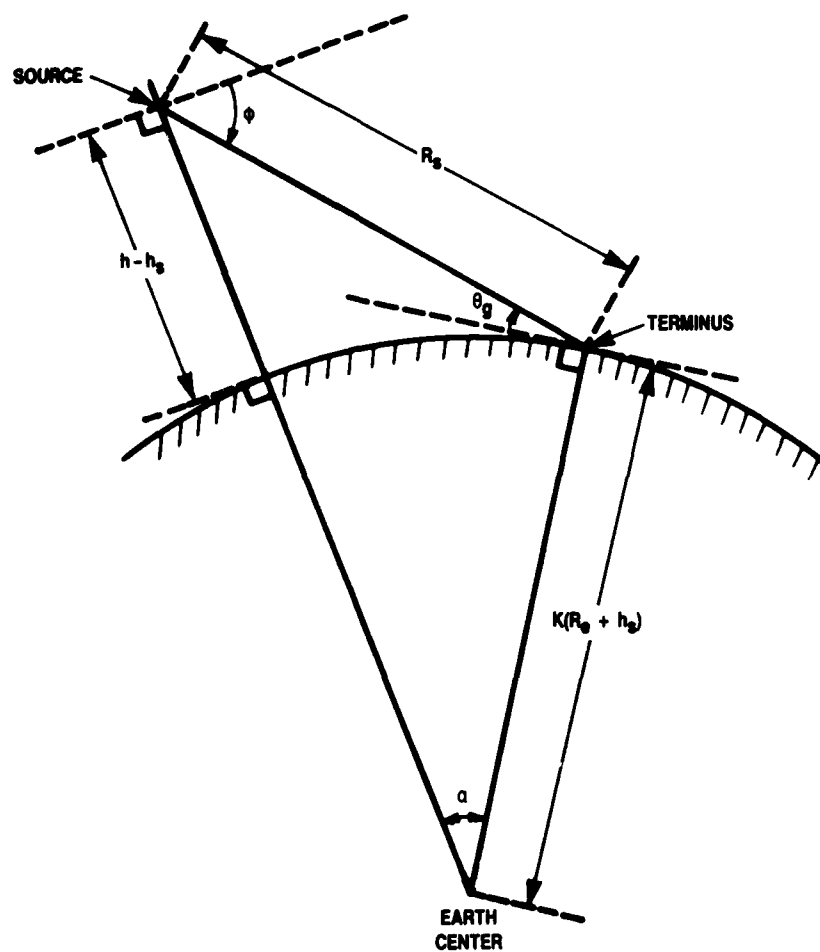


Figure 2. Effective Earth Radius Geometry

$$R_g = K(R_e + h_s) \sin^{-1} \left[ \frac{R_s \cos \phi}{K(R_e + h_s)} \right] \quad (13)$$

$$\theta_g = -\alpha - \phi \quad (14)$$

For paths within one kilometer of the surface, the correct scale factor is a function of the refractivity at the surface ( $N_s$ ), which establishes the gradient (see appendix), and under ideal conditions, is given by the convenient expression:<sup>3</sup>

$$K = \left[ 1 - 0.04665e^{0.005577N_s} \right]^{-1} \quad (15)$$

The often quoted  $K = 4/3$  corresponds to  $N_s \cong 301$ . Surface refractivity typically lies between 200 and 400 N-units.

Calculation of the ground range and slant range to the radio horizon is simple, since at the horizon  $\theta_g = 0$  and  $\alpha = -\phi$ , i.e., the triangle of figure 2 is a right triangle. The ranges for propagation to the horizon are,

$$R_{s, \text{horz.}} = \left[ (h - h_s) [2KR_e + (2K - 1)h_s + h] \right]^{\frac{1}{2}} \quad (16)$$

$$R_{g, \text{horz.}} = K(R_e + h_s) \sec^{-1} \left[ 1 + \frac{h - h_s}{K(R_e + h_s)} \right] \quad (17)$$

while the corresponding elevation angle at the source is:

$$\phi = -\sec^{-1} \left[ 1 + \frac{h - h_s}{K(R_e + h_s)} \right] \quad (18)$$

The EERM greatly simplifies atmospheric propagation geometry and it provides a good approximation for propagation path parameters if the proper scale factor is used as is discussed in the next section. As noted previously,  $K = 4/3$  is sometimes employed as a general rule of thumb -- often without sufficient justification. In section 3, results produced by the ray trace model are used to determine the altitude dependence of  $K$  and the accuracy of the EERM for higher altitude paths.

### SECTION 3

#### RESULTS: A COMPARISON OF RAY TRACE AND EERM PREDICTIONS

Ray trace computations based on the concentric shell atmospheric model have been performed using an HP-41CV system. Input variables are:

1. Source Altitude (MSL)
2. Terrain (Surface) Altitude (MSL)
3. Ray (beam) Initial Elevation (or Depression) Angle
4. Refractivity at the Surface ( $N_s$ )
5. Number of Shells (M)
6. Thickness of Lowest Shell ( $\Delta h$ )

From 80 to 100 shells between the source and surface were sufficient, as judged by the observed rapid convergence of the ray trace algorithm. The variation of shell thickness was chosen to be roughly in inverse proportion to the range of the refractivity gradient from the source to surface so that the thinnest shells were always near the surface.

Ray trace program outputs included:

1. Spatial Slant Range (equation 9)
2. Ground Range
3. Earth Grazing Angle

In tables 1, 2, and 3, ground ranges and grazing angles obtained from ray trace calculations are displayed for source altitudes of 15 kft., 45 kft., and 60 kft, respectively. All of these cases are based on a terrain altitude of 1 kft. and surface refractivity of 300 N-units. As the initial ray depression is decreased, the ground range increases and grazing angle decreases as expected. Included for comparison in these tables are the corresponding EERM results obtained with scale factors of 1.209, 1.116 and 1.089 for tables 1, 2 and 3, respectively. The EERM fit to the ray trace results was enforced at a ground range value of 80% of the EERM predicted radio horizon ground range. For example, in table 1 the EERM radio horizon lies at a

Table 1

Model Comparison for Source at 15 kft.,  
Surface at 1 kft. and  $N_s = 300$

DEPRESSION ANGLE AT SOURCE	RAY TRACE MODEL		EFFECTIVE EARTH RADIUS MODEL (K = 1.209)	
	$R_g$ (km)	$\theta_g^\circ$	$R_g$ (km)	$\theta_g^\circ$
5°	50.71	4.63°	50.68	4.62°
3°	92.05	2.32°	91.88	2.32°
2.4°	127.06	1.47°	126.65	1.46°
2.1°	164.62	0.90°	163.95	0.88°
1.96°	202.44	0.50°	202.35	0.46°
1.92°	224.62	0.30°	227.52	0.23°
1.906°	238.16	0.19°	256.38	0°
1.897°	256.43	0.05°	--	--

Table 2

Model Comparison for Source at 45 kft.,  
Surface at 1 kft. and  $N_s = 300$

ELEVATION AT SOURCE	RAY TRACE MODEL		EFFECTIVE EARTH RADIUS MODEL ( $K = 1.116$ )	
	$R_g$ (km)	$\theta_g^\circ$	$R_g$ (km)	$\theta_g^\circ$
8°	100.57	7.2°	100.48	7.19°
5°	179.58	3.58°	179.08	3.56°
4.3°	227.21	2.51°	226.26	2.48°
4.0°	260.87	1.95°	259.58	1.91°
3.8°	294.10	1.50°	292.60	1.44°
3.6°	350.93	0.88°	350.71	0.77°
3.516°	403.22	0.42°	436.44	0
3.492°	447.73	0.06°	--	--

Table 3

Model Comparison for Source at 60 kft.,  
Surface at 1 kft. and  $N_s = 300$

DEPRESSION ANGLE AT SOURCE	RAY TRACE MODEL		EFFECTIVE EARTH RADIUS MODEL ( $K = 1.089$ )	
	$R_g$ (km)	$\theta_g^\circ$	$R_g$ (km)	$\theta_g^\circ$
10°	106.72	9.13°	106.64	9.12°
7°	162.14	5.69°	161.84	5.66°
5°	263.33	2.88°	262.23	2.84°
4.6°	310.72	2.11°	309.20	2.05°
4.35°	359.20	1.49°	357.75	1.40°
4.23°	396.36	1.09°	396.25	0.96°
4.12°	459.60	0.51°	499.09	0°
4.089°	513.44	0.08°	--	--

ground range of 256.38 km, and the EERM scale factor was chosen to produce agreement at ~200 km as can be seen for the fifth table entry. Since the EERM horizon distance is itself dependent upon the scale factor, several manual iterations were required to obtain the desired fit. Any attempt to fit the EERM to the ray trace results involves a compromise between the agreement obtainable at high and lower ranges. The procedure described gives very satisfactory agreement for ranges out to 85% of the radio horizon, and fair to bad agreement over the remaining interval. A fit to ranges near the horizon would produce poor agreement at intermediate ranges. It is interesting to note that the ray trace and EERM horizon ground ranges are in relatively good agreement as can be gleaned from the lowest entries in tables 1, 2, and 3.

Comparison of ray trace and EERM predictions is far more striking when displayed in the format of figures 3, 4, and 5, in which spatial slant range is plotted against initial depression angle. For the relatively shallow depression angles spanned by the figures, little accuracy would be lost if "ground range" were substituted for "slant range" along the ordinate, since the rays are roughly parallel to the ground. The fitted values ( $K = 1.209$ , figure 3;  $1.116$ , figure 4;  $1.089$ , figure 5) conform impressively to the ray trace results, while the "overused"  $4/3$  value is clearly inferior in each case. The  $K = 1$  plots correspond to a line of sight (in vacuo) calculation. Note that  $K = 4/3$  is more accurate than  $K = 1$  for the low altitude source (figure 3) while  $K = 1$  is more accurate than  $K = 4/3$  for the high altitude source (figure 5) as expected.

In figure 6, earth grazing angle is plotted against initial depression angle for the 45 kft. source altitude case. Once again, the superiority of the accuracy obtained with the fitted scale factor is immediately evident.

These encouraging findings prompted a more thorough investigation of the scale factor's dependence on both source altitude and surface refractivity. Table 4 contains ray trace fitted  $K$  values at nine altitudes for each of three  $N_s$  values:  $N_s = 200$ , 300, and 400 N-units.

The low altitude case (4 kft.) of table 4 is of particular interest, since the propagation path lies entirely within the linear region of the refractivity profile, which, in the semi-empirical model, extends to 1 km (3.3 kft.) above the surface. Thus, for this case the ray trace model fitted scale factors should corroborate the prediction of equation (15), which is based on analytical work. Indeed, the tabular values  $1.165$  ( $N_s = 200$ ),  $1.327$  ( $N_s = 300$ ) and  $1.756$  ( $N_s = 400$ )



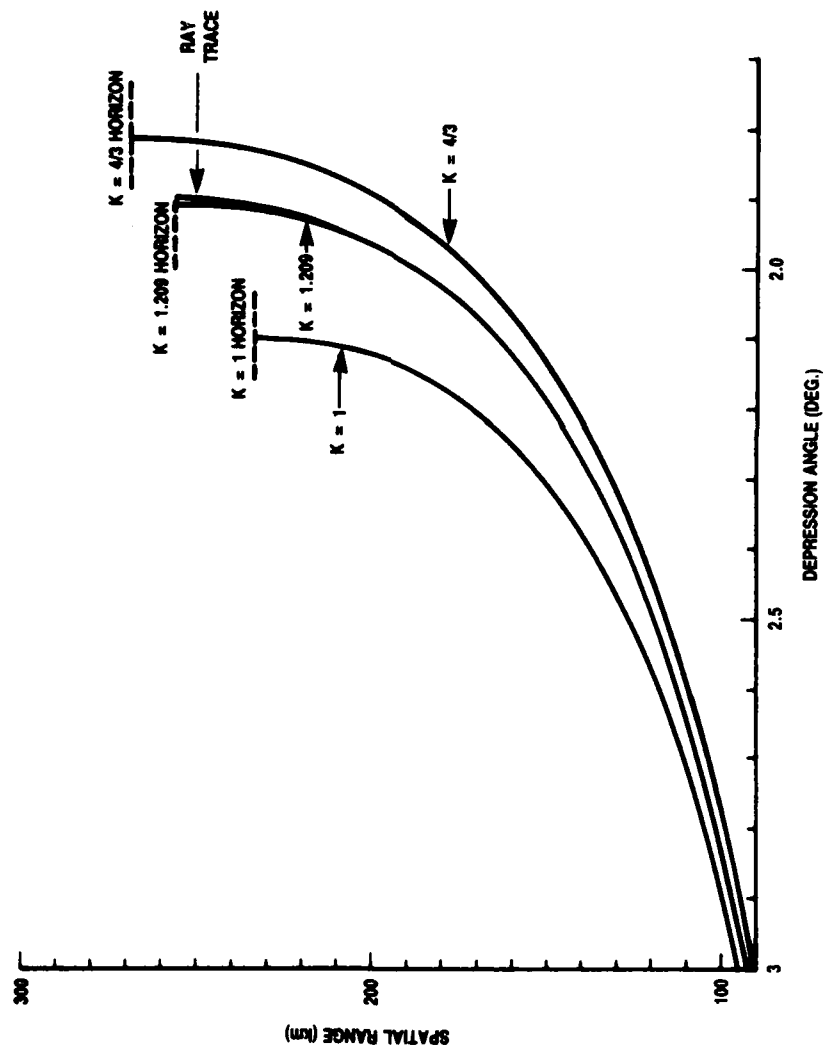


Figure 3. Range Versus Initial Depression Angle for Source at 15 kft., Terrain Elevation of 1 kft. and  $N_s = 300$

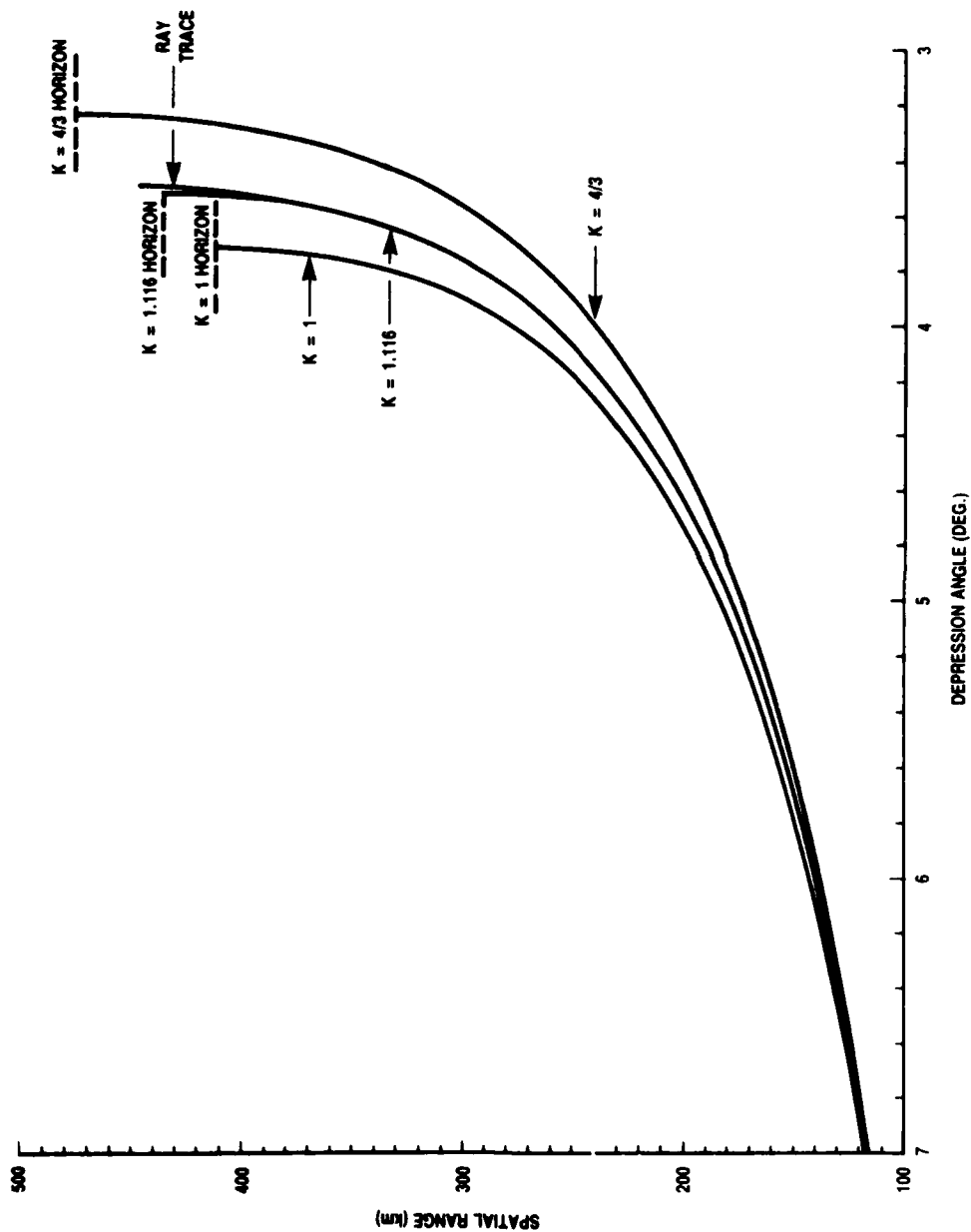


Figure 4. Range Versus Initial Depression Angle for Source at 45 kft., Terrain Elevation of 1 kft. and  $N_s = 300$

1A-47,444

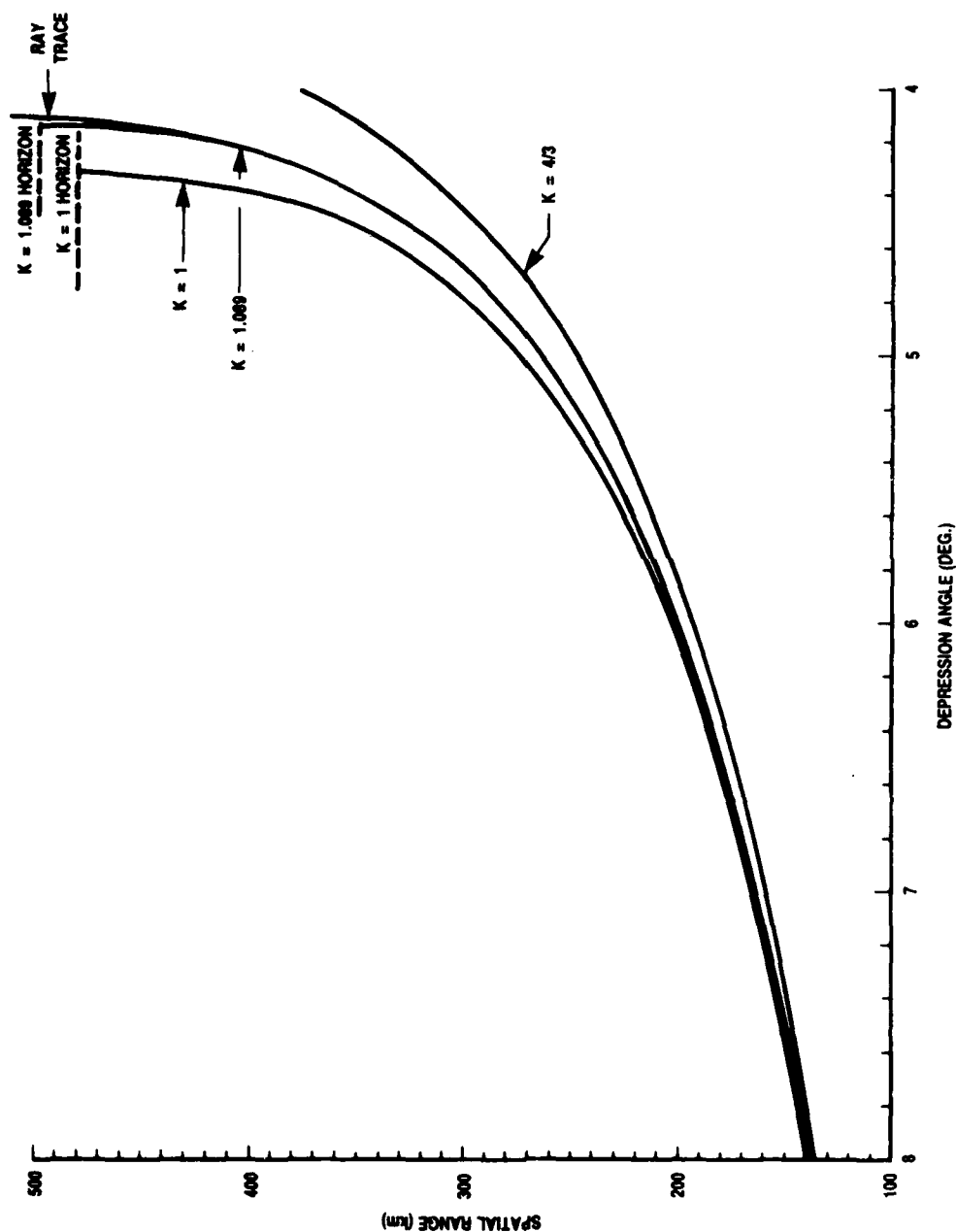


Figure 5. Range Versus Initial Depression Angle for Source at 60 kft., Terrain Elevation of 1 kft. and  $N_s = 300$

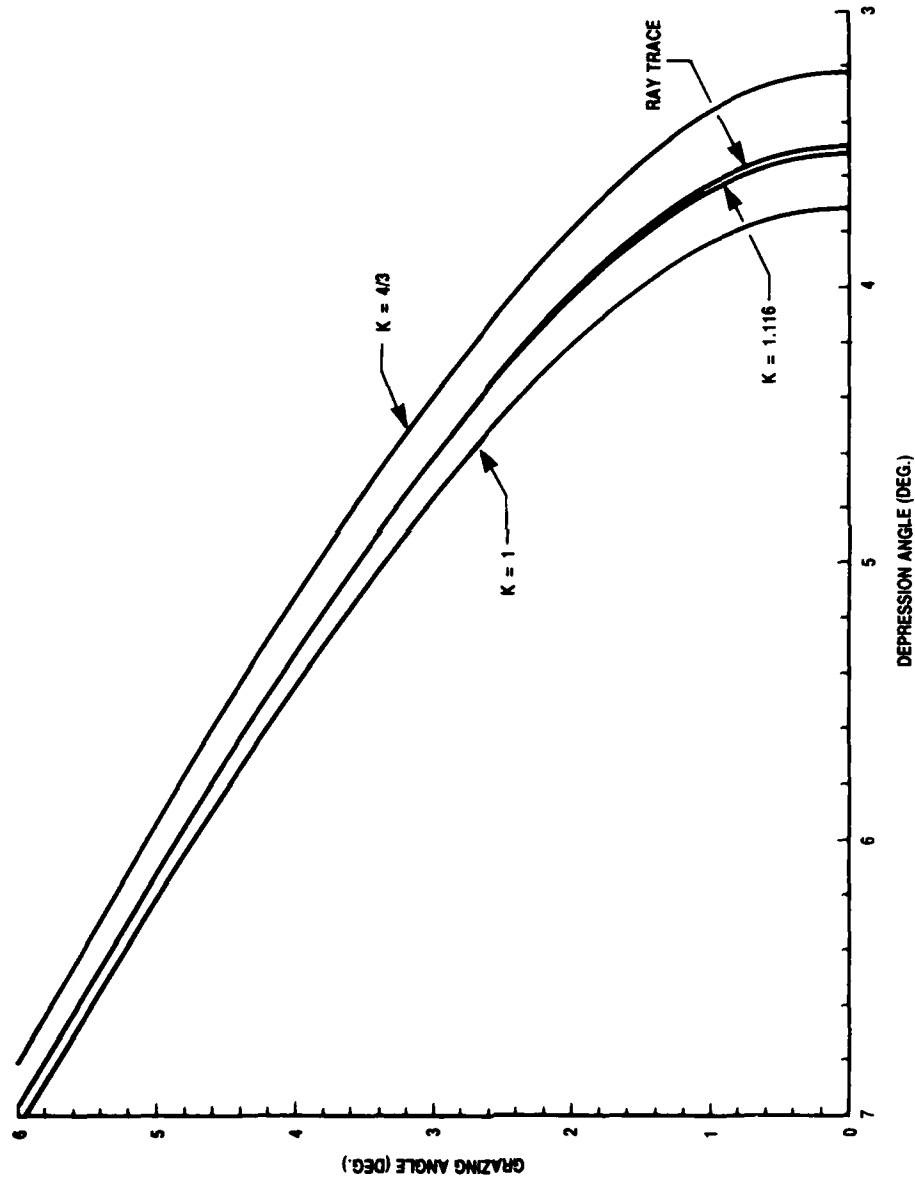


Figure 6. Grazing Angle Versus Depression Angle for Source at 45 kft., Terrain Elevation of 1 kft. and  $N_s = 300$

Table 4

Effective Earth Radius Factor Versus Source Altitude  
and Surface Refractivity For 1 kft. Terrain Elevation

SOURCE ALTITUDE kft. (MSL)	EARTH RADIUS FACTOR (K)		
	$N_s = 200$	$N_s = 300$	$N_s = 400$
4	1.165	1.327	1.756
8	1.111	1.261	1.520
15	1.086	1.209	1.371
30	1.067	1.149	1.233
38	1.072	1.130	1.188
45	1.069	1.116	1.159
60	1.059	1.089	1.115
75	1.049	1.071	1.090
90	1.041	1.056	1.071

are in excellent agreement with the equation (15) derived values of 1.166, 1.331 and 1.767, respectively - a result which underscores the accuracy of the ray trace model.

Figure 7 displays smooth curves of scale factor versus source altitude for targets or receivers on 1 kft. terrain. These functions were obtained via a manual fit to the plotted reference points of table 4. For  $N_s = 400$  and 300, the scale factor decreases monotonically with increasing source altitude as anticipated, while for  $N_s = 200$ , a relatively flat region appears between 30 kft. and 50 kft. altitude. The unusual variation of  $K$  for the latter case can be understood as a consequence of the refractivity model employed in the calculations. The bending power of the atmosphere is proportional to the magnitude of the refractivity gradient, not the absolute refractivity. As seen in figure A-3, the gradient for the  $N_s = 200$  case displays a sharp discontinuity at 9 km, which indicates that the bending power of the atmosphere is larger over a wide range of higher altitudes than it is at lower altitudes. This accounts for the flat spot in the  $N_s = 200$  curve of figure 7.

The scale factors tend to converge for high altitude sources since  $N_s$  influences the refractivity profile only up to altitudes of 9 km (see appendix).

As noted earlier, the EERM-ray trace agreement degrades near the radio horizon. This trend is illustrated in figures 8 and 9, which display EERM ground range plotted against ray trace model ground range for common values of depression angle. Deviations from a 45° line through the origin indicate discrepancies, and it is seen that in the horizon region the EERM consistently predicts ground ranges which are somewhat longer than those predicted by the ray trace model. This result is a consequence of the exponential refractivity altitude dependence used in the ray trace work. Bending in the lower atmosphere is accentuated, causing ground range to fall short of the EERM predictions. Note that for the 4 km source altitude case of figure 9, no discrepancy is evident, since the model refractivity gradient is constant from the surface to 1 km (3.3. kft.).

The departure of the EERM approximation from the ray trace prediction near the radio horizon for the fitted scale factors is not especially disturbing, since no model can be expected to produce consistently accurate predictions in this region, under ordinary circumstances anyway. In the horizon region irregularities in the refractivity structure are magnified as a result of low grazing angles (e.g., consider highway mirages seen at low grazing angles over hot pavement). As a practical rule, the EERM predictions may be regarded as good approximations, when atmospheric irregularities are not large,

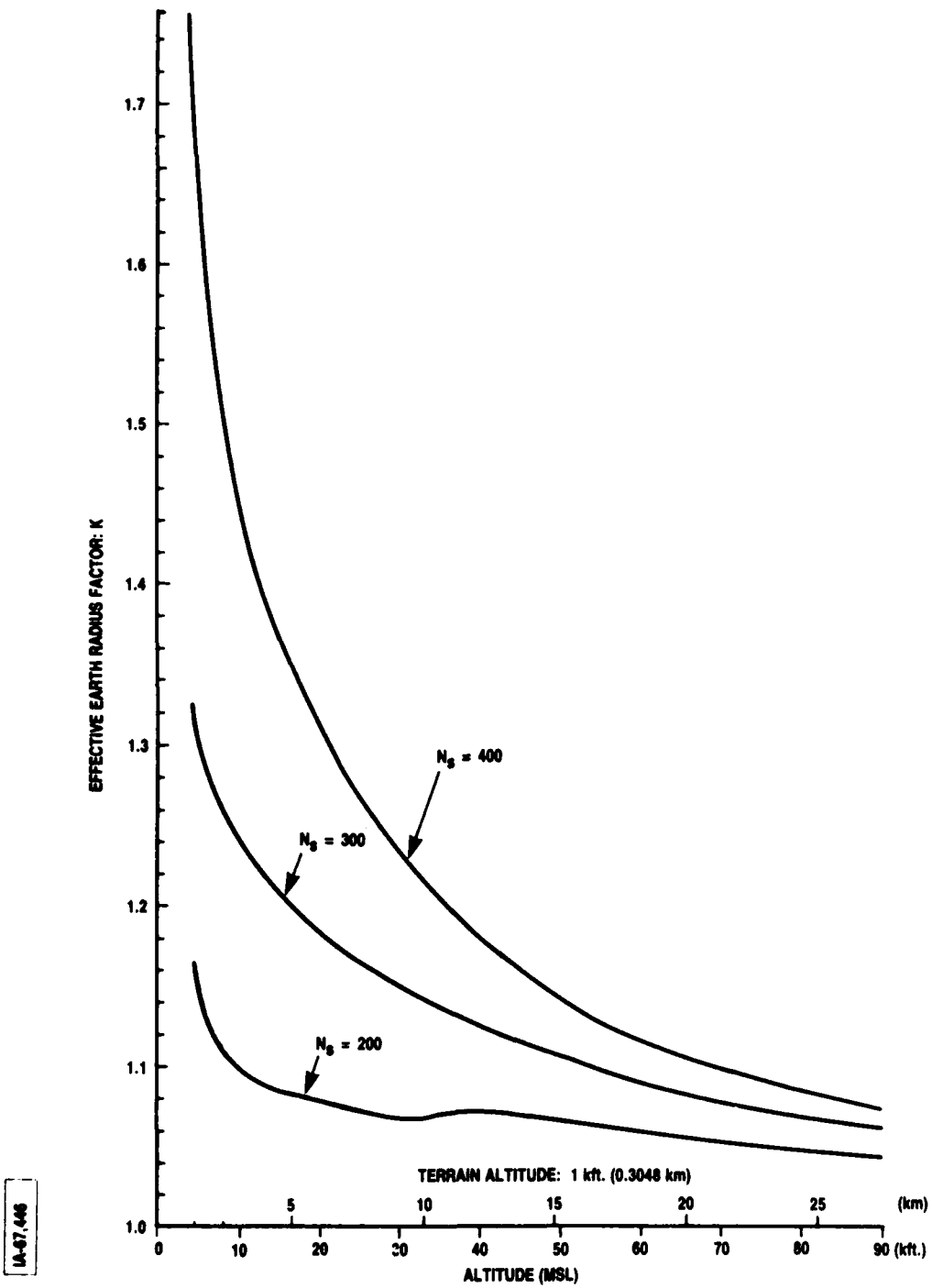
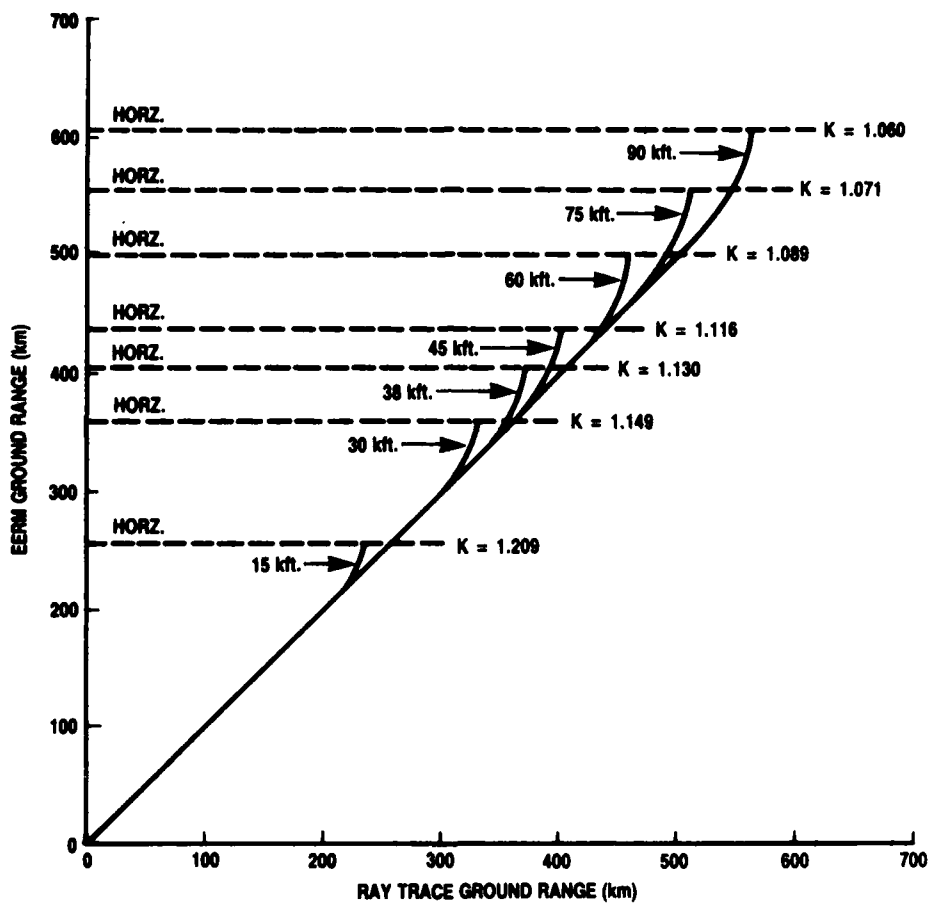


Figure 7. Effective Earth Radius Factor Versus Source Altitude for  $N_s = 200, 300$  and  $400$



1A-87,447

Figure 8. Ray Trace Versus Effective Earth Radius  
Model Ground Range for Higher Altitude Paths



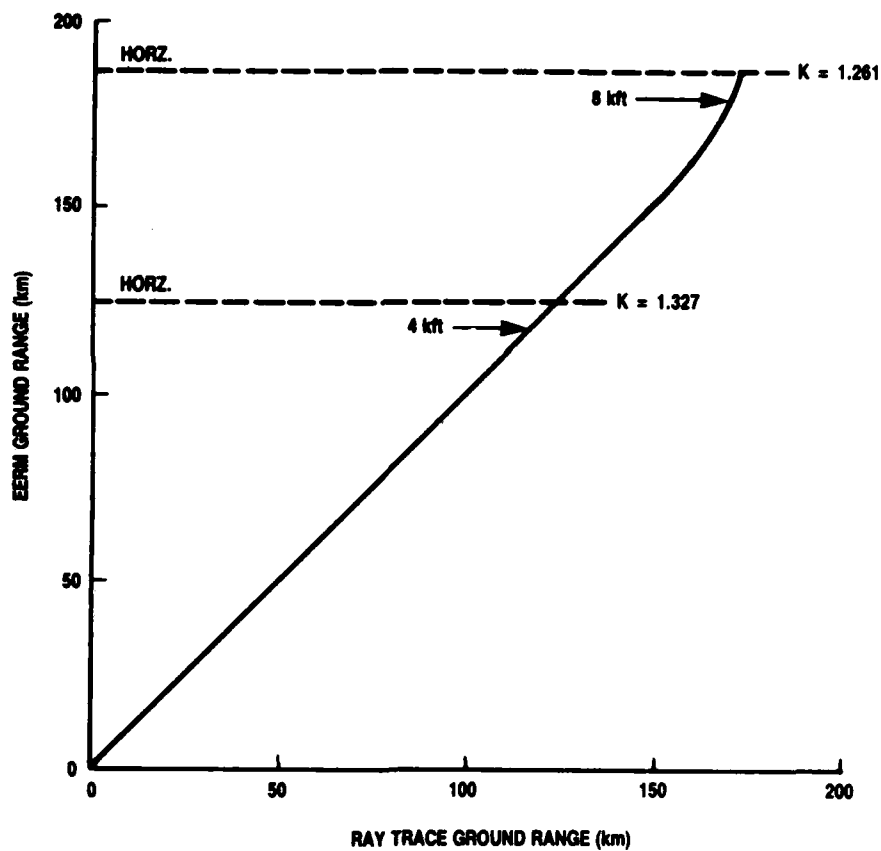


Figure 9. Ray Trace Versus Effective Earth Radius  
Model Ground Range for Lower Altitude Paths

for ranges up to 85% of the horizon distance at higher altitudes (90 kft.  $> h > 60$  kft.) and for ranges up to 90% of the horizon distance for lower altitudes (4 kft.  $\leq h < 60$  kft.).

The results presented thus far apply for a surface altitude of 1 kft., which was chosen as a nominal value. Table 5 displays a set of scale factors which were determined for the same conditions as those of table 4, save for a specified surface elevation of 2 kft. (0.61 km). For high altitude sources, the scale factor changes very little (compare, table 4) while for intermediate and low-intermediate source altitudes, changes are more significant but still unremarkable. For the lowest altitude case (4 km), no change in scale factor is seen, since in the linear profile region the scale factor does not depend on the source-surface altitude difference. In the context of the present atmospheric model, the change in surface altitude is approximately equivalent to an equal and opposite change in source altitude. From the slopes of the curves of figure 7, it is then evident that the scale factor will vary more strongly for the lower altitude points (save for the lowest) when the surface altitude is changed.

Table 5

Effective Earth Radius Factor Versus Source Altitude  
and Surface Refractivity For 2 kft. Terrain Elevation

SOURCE ALTITUDE kft. (MSL)	EARTH RADIUS FACTOR (K)		
	$N_s = 200$	$N_s = 300$	$N_s = 400$
4	1.165	1.327	1.756
8	1.120	1.278	1.568
15	1.091	1.222	1.401
30	1.070	1.156	1.243
38	1.074	1.134	1.194
45	1.071	1.118	1.162
60	1.060	1.090	1.116
75	1.049	1.070	1.090
90	1.040	1.057	1.070

## SECTION 4

### CONCLUSIONS

The effective earth radius method (EERM), which is rigorous for propagation in atmospheres with a linear refractivity profile (constant gradient), has been extended to higher propagation paths for which the refractivity decreases exponentially with altitude. The extension is based on ray trace computations which treat the earth's atmosphere as a collection of concentric shells whose refractive indices are assigned in accordance with a semi-empirical model.<sup>4</sup>

The popular 4/3 EERM scale factor is only appropriate for propagation paths within 1 km (3.3 kft.) of the surface when the ground level refractivity is near the "average" value of 300 N-units. For higher altitude paths, significantly smaller scale factors than those obtained from calculations in the low altitude region are indicated by the ray trace results. Appropriate scale factors have been computed for source altitudes from 4 kft. to 90 kft., for surface refractivities of 200, 300, and 400 N-units (tables 4 and 5). Interpolation may be used to estimate scale factors for intermediate cases.

As a cautionary note, it must be emphasized that the use of average or idealized atmospheric refractivity models, while permitting computational simplicity, does not do justice to the real complexity and variability of the atmosphere - particularly the troposphere. Model calculations based on such idealized conditions should be used only when more detailed data are unavailable, or for overall convenience when accuracy is not crucial.

Ground range estimates obtained from the extended EERM can not be expected to have high accuracy for basically 2 reasons:

1. The EERM is only an approximation to the ray trace results for altitudes above 1 km.
2. The ray trace results themselves are based on a model atmosphere which only reflects average conditions.

If high accuracy is required, ray trace analysis must be performed in the context of a realistic model atmosphere tailored to the area of interest.

#### LIST OF REFERENCES

1. R. S. White, Space Physics, (Gordon and Breach, 1970) pg. 61-64.
2. F. E. Nathanson, Radar Design Principles, (McGraw-Hill, 1969) pg. 28-33.
3. W. C. Jakes, ed., Microwave Mobile Communications, (John Wiley and Sons, 1974) pg. 84-85.
4. M. I. Skolnik, Radar Handbook, (McGraw-Hill, 1970) pg. 24-10.

## APPENDIX

### SEMI-EMPIRICAL ATMOSPHERIC REFRACTIVITY MODEL

The refractivity of the earth's atmosphere can, on the average, be represented by the model described below, which is taken directly from the Radar Handbook.<sup>4</sup>

The atmosphere is assumed to be stratified, i.e., it is uniform at a given altitude, with respect to latitude and longitude over the earth's surface. The model refractivity is a function of only three variables:

1. Altitude above mean sea level;  $h$
2. Terrain elevation above mean sea level;  $h_s$
3. Refractivity at the surface ( $h = h_s$ );  $N_s$

Three altitude regions are defined by the refractivity model.

1. The linear region
2. The surface refractivity and surface altitude dependent exponential region
3. The fixed exponential region

Each of these regions is described quantitatively below.

#### A. The Linear Region

Within one kilometer (3.3 kft.) of the earth's surface the refractivity is assumed to decrease linearly with altitude. This is, therefore, the region in which the effective earth radius model is rigorous and in which the scale factor is, therefore, independent of altitude. The refractivity is given by,

$$N = N_s + \Delta N(h - h_s) ; \quad h_s \leq h \leq h_s + 1(\text{km}) \quad (\text{A-1})$$

in which,

$$\Delta N = -7.32 \exp(0.005577 N_s) \quad (\text{A-2})$$

is the magnitude of the refractivity gradient, which is constant in this region for a given surface refractivity.

#### B. The $N_s$ and $h_s$ Dependent Exponential Region

Between the top of the linear region ( $h_s + 1$  km) and 9 km altitude, the refractivity profile is assumed to be exponential. The function must be continuous at the boundary with the linear region and must give  $N = 105$  at 9 km. The continuity requirement forces the exponential decay constant to be dependent upon both  $N_s$  and  $h_s$ . The refractivity is given by,

$$N = N_1 \exp[C(h - h_s - 1)] ; \quad h_s + 1 \leq h \leq 9(\text{km}) \quad (\text{A-3})$$

in which,

$$C = \left( \frac{1}{h_s - 8} \right) \ln \left( \frac{N_1}{105} \right) \quad (\text{A-4})$$

and,

$$N_1 = N_s + \Delta N \quad (\text{A-5})$$

The magnitude of the refractivity gradient is also exponential and is given by,

$$\frac{\partial N}{\partial h} = CN = CN_1 \exp[C(h - h_s - 1)] \quad (\text{A-6})$$

and is not, in general, continuous at the upper and lower boundaries of this region.

### C. The Fixed Exponential Region

The refractivity profile is exponential in the third, uppermost region, and is independent of surface conditions. The decay constant is fixed and the refractivity is 105 N-units at the lower boundary:

$$N = 105 \exp[0.1424(9 - h)] ; \quad 9 \leq h(\text{km}) \quad (\text{A-7})$$

The magnitude of the refractivity gradient is,

$$\frac{\partial N}{\partial h} = -14.952 \exp[0.1424(9 - h)] \quad (\text{A-8})$$

Figures A-1 and A-2 contain plots of refractivity versus altitude for a surface elevation of 1 kft. (0.3048 km) and surface refractivities of 200, 300 and 400 N-units. Figure A-3 contains the corresponding plots of the refractivity gradient, in which the discontinuities at 1.30 and 9 km are clearly indicated. Although discontinuities of this type are unphysical, any model of the atmosphere must make compromises somewhere, and in this case the gradient has anomalies for the sake of maintaining the simplicity of the profile.



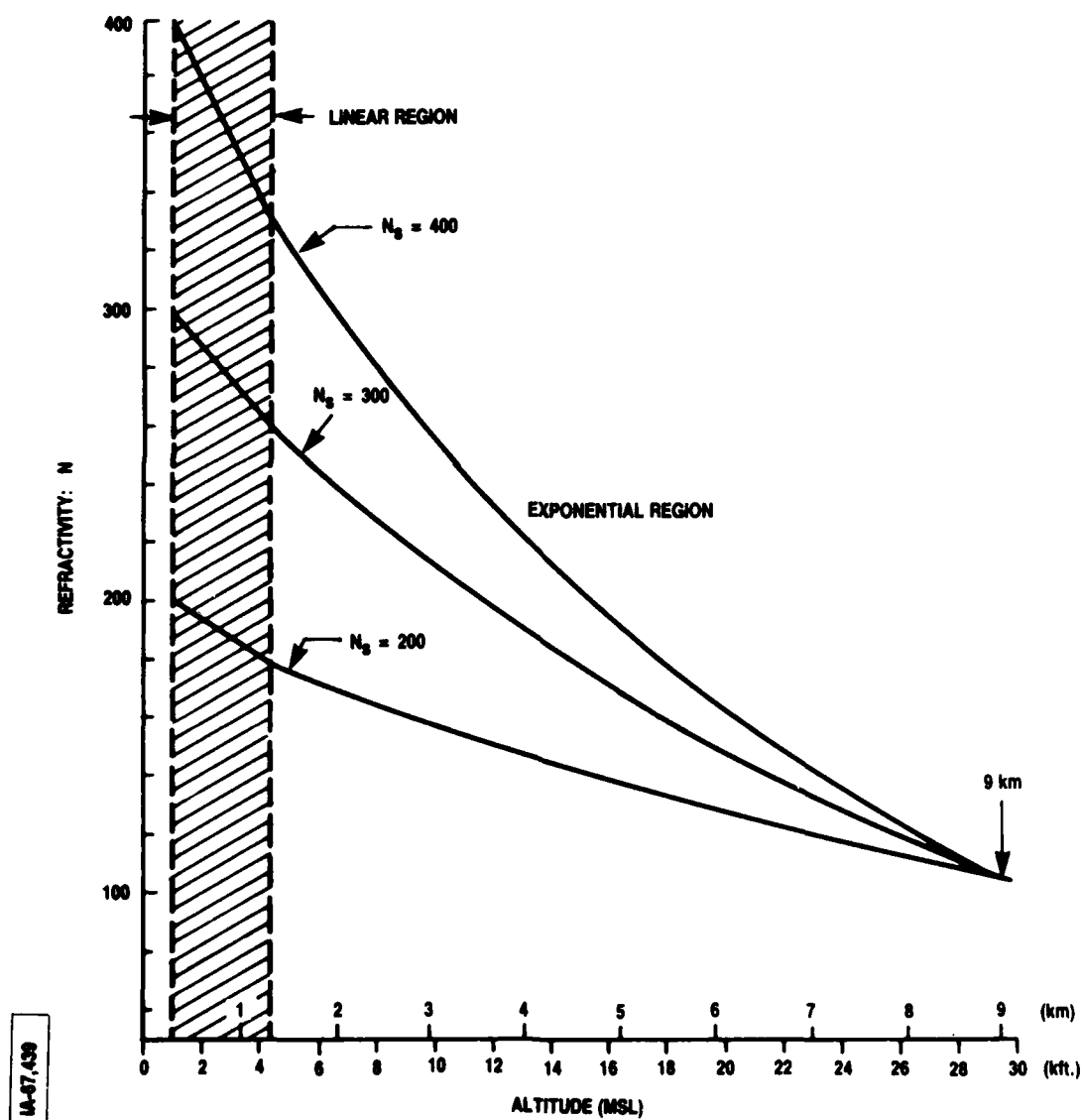


Figure A-1. Refractivity Profiles: 1-30 kft. MSL

1A-67,440

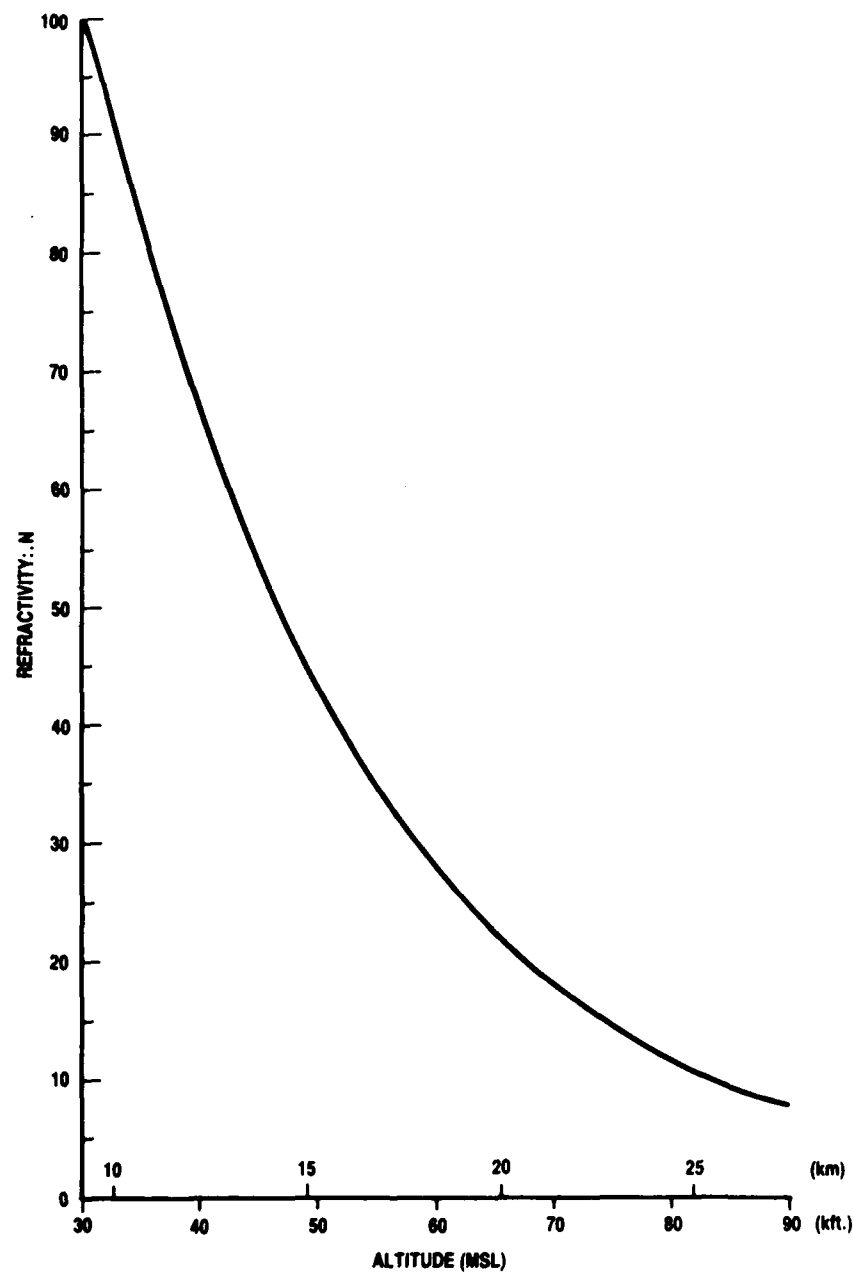


Figure A-2. Refractivity Profile: 30-90 kft. MSL

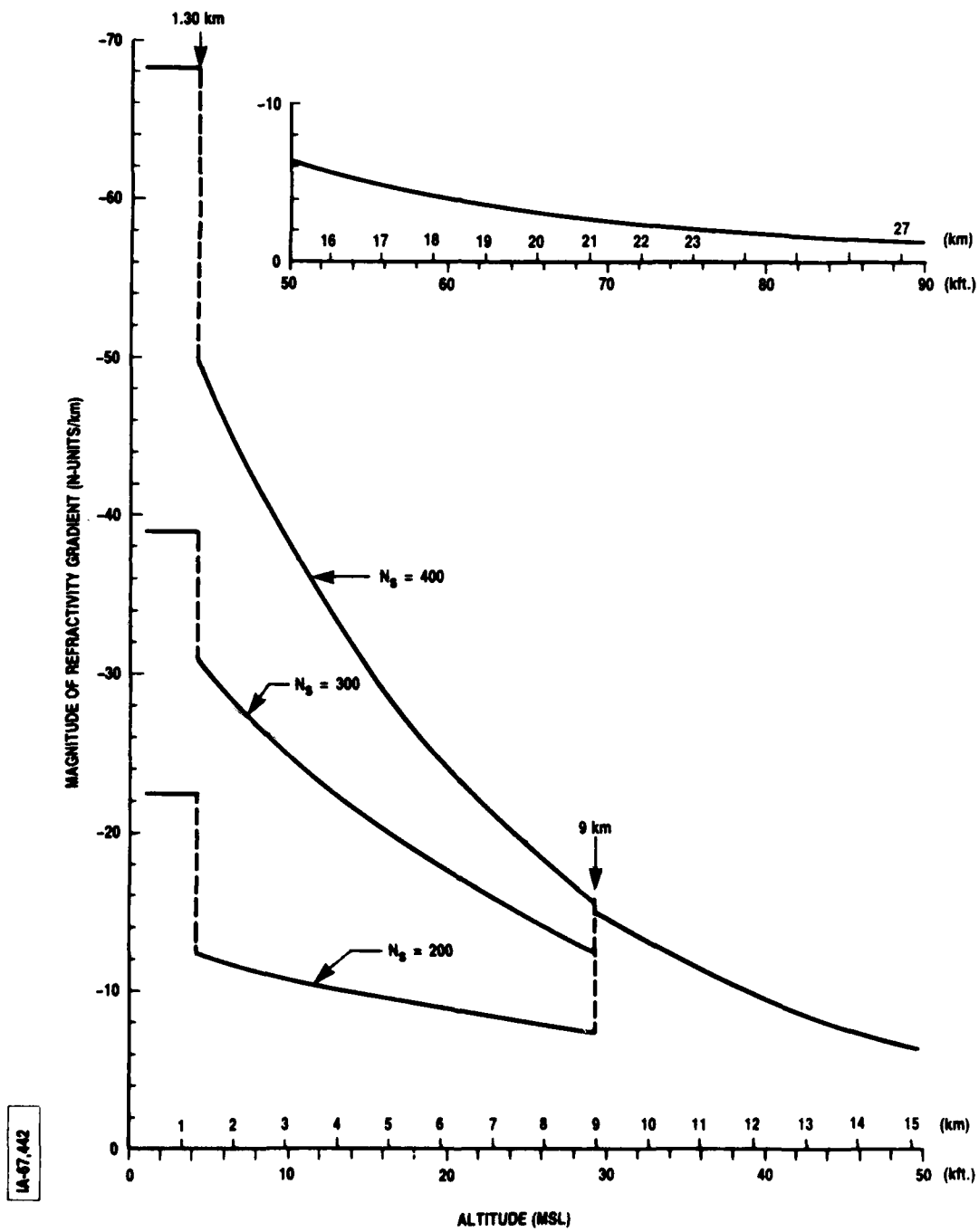


Figure A-3. Refractivity Gradient Versus Altitude

END

FILMED

2-84

DTIC